

Measurement of the Lifetime Difference between B_s Mass Eigenstates

- D. Acosta,¹⁶ J. Adelman,¹² T. Affolder,⁹ T. Akimoto,⁵⁴ M. G. Albrow,¹⁵ D. Ambrose,⁴³ S. Amerio,⁴² D. Amidei,³³
 A. Anastassov,⁵⁰ K. Anikeev,¹⁵ A. Annovi,⁴⁴ J. Antos,¹ M. Aoki,⁵⁴ G. Apollinari,¹⁵ T. Arisawa,⁵⁶ J-F. Arguin,³²
 A. Artikov,¹³ W. Ashmanskas,¹⁵ A. Attal,⁷ F. Azfar,⁴¹ P. Azzi-Bacchetta,⁴² N. Bacchetta,⁴² H. Bachacou,²⁸ W. Badgett,¹⁵
 A. Barbaro-Galtieri,²⁸ G. J. Barker,²⁵ V. E. Barnes,⁴⁶ B. A. Barnett,²⁴ S. Baroiant,⁶ M. Barone,¹⁷ G. Bauer,³¹ F. Bedeschi,⁴⁴
 S. Behari,²⁴ S. Belforte,⁵³ G. Bellettini,⁴⁴ J. Bellinger,⁵⁸ E. Ben-Haim,¹⁵ D. Benjamin,¹⁴ A. Beretvas,¹⁵ A. Bhatti,⁴⁸
 M. Binkley,¹⁵ D. Bisello,⁴² M. Bishai,¹⁵ R. E. Blair,² C. Blocker,⁵ K. Bloom,³³ B. Blumenfeld,²⁴ A. Bocci,⁴⁸ A. Bodek,⁴⁷
 G. Bolla,⁴⁶ A. Bolshov,³¹ P. S. L. Booth,²⁹ D. Bortoletto,⁴⁶ J. Boudreau,⁴⁵ S. Bourov,¹⁵ B. Brau,⁹ C. Bromberg,³⁴
 E. Brubaker,¹² J. Budagov,¹³ H. S. Budd,⁴⁷ K. Burkett,¹⁵ G. Busetto,⁴² P. Bussey,¹⁹ K. L. Byrum,² S. Cabrera,¹⁴
 M. Campanelli,¹⁸ M. Campbell,³³ A. Canepa,⁴⁶ M. Casarsa,⁵³ D. Carlsmith,⁵⁸ S. Carron,¹⁴ R. Carosi,⁴⁴ M. Cavalli-Sforza,³
 A. Castro,⁴ P. Catastini,⁴⁴ D. Cauz,⁵³ A. Cerri,²⁸ L. Cerrito,²³ J. Chapman,³³ C. Chen,⁴³ Y. C. Chen,¹ M. Chertok,⁶
 G. Chiarelli,⁴⁴ G. Chlachidze,¹³ F. Chlebana,¹⁵ I. Cho,²⁷ K. Cho,²⁷ D. Chokheli,¹³ J. P. Chou,²⁰ M. L. Chu,¹ S. Chuang,⁵⁸
 J. Y. Chung,³⁸ W-H. Chung,⁵⁸ Y. S. Chung,⁴⁷ C. I. Ciobanu,²³ M. A. Ciocci,⁴⁴ A. G. Clark,¹⁸ D. Clark,⁵ M. Coca,⁴⁷
 A. Connolly,²⁸ M. Convery,⁴⁸ J. Conway,⁶ B. Cooper,³⁰ M. Cordelli,¹⁷ G. Cortiana,⁴² J. Cranshaw,⁵² J. Cuevas,¹⁰
 R. Culbertson,¹⁵ C. Currat,²⁸ D. Cyr,⁵⁸ D. Dagenhart,⁵ S. Da Ronco,⁴² S. D'Auria,¹⁹ P. de Barbaro,⁴⁷ S. De Cecco,⁴⁹
 G. De Lentdecker,⁴⁷ S. Dell'Agnello,¹⁷ M. Dell'Orso,⁴⁴ S. Demers,⁴⁷ L. Demortier,⁴⁸ M. Deninno,⁴ D. De Pedis,⁴⁹
 P. F. Derwent,¹⁵ C. Dionisi,⁴⁹ J. R. Dittmann,¹⁵ C. Dörr,²⁵ P. Doksyk,²³ A. Dominguez,²⁸ S. Donati,⁴⁴ M. Donega,¹⁸
 J. Donini,⁴² M. D'Onofrio,¹⁸ T. Dorigo,⁴² V. Drollinger,³⁶ K. Ebina,⁵⁶ N. Eddy,²³ J. Ehlers,¹⁸ R. Ely,²⁸ R. Erbacher,⁶
 M. Erdmann,²⁵ D. Errede,²³ S. Errede,²³ R. Eusebi,⁴⁷ H-C. Fang,²⁸ S. Farrington,²⁹ I. Fedorko,⁴⁴ W. T. Fedorko,¹²
 R. G. Feild,⁵⁹ M. Feindt,²⁵ J. P. Fernandez,⁴⁶ C. Ferretti,³³ R. D. Field,¹⁶ G. Flanagan,³⁴ B. Flaughier,¹⁵
 L. R. Flores-Castillo,⁴⁵ A. Foland,²⁰ S. Forrester,⁶ G. W. Foster,¹⁵ M. Franklin,²⁰ J. C. Freeman,²⁸ Y. Fujii,²⁶ I. Furic,¹²
 A. Gajjar,²⁹ A. Gallas,³⁷ J. Galyardt,¹¹ M. Gallinaro,⁴⁸ M. Garcia-Sciveres,²⁸ A. F. Garfinkel,⁴⁶ C. Gay,⁵⁹ H. Gerberich,¹⁴
 D. W. Gerdes,³³ E. Gerchtein,¹¹ S. Giagu,⁴⁹ P. Giannetti,⁴⁴ A. Gibson,²⁸ K. Gibson,¹¹ C. Ginsburg,⁵⁸ K. Giolo,⁴⁶
 M. Giordani,⁵³ M. Giunta,⁴⁴ G. Giurgiu,¹¹ V. Glagolev,¹³ D. Glenzinski,¹⁵ M. Gold,³⁶ N. Goldschmidt,³³ D. Goldstein,⁷
 J. Goldstein,⁴¹ G. Gomez,¹⁰ G. Gomez-Ceballos,¹⁰ M. Goncharov,⁵¹ O. González,⁴⁶ I. Gorelov,³⁶ A. T. Goshaw,¹⁴
 Y. Gotra,⁴⁵ K. Goulianatos,⁴⁸ A. Gresele,⁴ M. Griffiths,²⁹ C. Grossi-Pilcher,¹² U. Grundler,²³ M. Guenther,⁴⁶
 J. Guimaraes da Costa,²⁰ C. Haber,²⁸ K. Hahn,⁴³ S. R. Hahn,¹⁵ E. Halkiadakis,⁴⁷ A. Hamilton,³² B-Y. Han,⁴⁷ R. Handler,⁵⁸
 F. Happacher,¹⁷ K. Hara,⁵⁴ M. Hare,⁵⁵ R. F. Harr,⁵⁷ R. M. Harris,¹⁵ F. Hartmann,²⁵ K. Hatakeyama,⁴⁸ J. Hauser,⁷ C. Hays,¹⁴
 H. Hayward,²⁹ E. Heider,⁵⁵ B. Heinemann,²⁹ J. Heinrich,⁴³ M. Hennecke,²⁵ M. Herndon,²⁴ C. Hill,⁹ D. Hirschbuehl,²⁵
 A. Hocker,⁴⁷ K. D. Hoffman,¹² A. Holloway,²⁰ S. Hou,¹ M. A. Houlden,²⁹ B. T. Huffman,⁴¹ Y. Huang,¹⁴ R. E. Hughes,³⁸
 J. Huston,³⁴ K. Ikado,⁵⁶ J. Incandela,⁹ G. Introzzi,⁴⁴ M. Iori,⁴⁹ Y. Ishizawa,⁵⁴ C. Issever,⁹ A. Ivanov,⁴⁷ Y. Iwata,²²
 B. Iyutin,³¹ E. James,¹⁵ D. Jang,⁵⁰ J. Jarrell,³⁶ D. Jeans,⁴⁹ H. Jensen,¹⁵ E. J. Jeon,²⁷ M. Jones,⁴⁶ K. K. Joo,²⁷ S. Y. Jun,¹¹
 T. Junk,²³ T. Kamon,⁵¹ J. Kang,³³ M. Karagoz Unel,³⁷ P. E. Karchin,⁵⁷ S. Kartal,¹⁵ Y. Kato,⁴⁰ Y. Kemp,²⁵ R. Kephart,¹⁵
 U. Kerzel,²⁵ V. Khotilovich,⁵¹ B. Kilminster,³⁸ D. H. Kim,²⁷ H. S. Kim,²³ J. E. Kim,²⁷ M. J. Kim,¹¹ M. S. Kim,²⁷
 S. B. Kim,²⁷ S. H. Kim,⁵⁴ T. H. Kim,³¹ Y. K. Kim,¹² B. T. King,²⁹ M. Kirby,¹⁴ L. Kirsch,⁵ S. Klimentko,¹⁶ B. Knuteson,³¹
 B. R. Ko,¹⁴ H. Kobayashi,⁵⁴ P. Koehn,³⁸ D. J. Kong,²⁷ K. Kondo,⁵⁶ J. Konigsberg,¹⁶ K. Kordas,³² A. Korn,³¹ A. Korytov,¹⁶
 K. Kotelnikov,³⁵ A. V. Kotwal,¹⁴ A. Kovalev,⁴³ J. Kraus,²³ I. Kravchenko,³¹ A. Kreymar,¹⁵ J. Kroll,⁴³ M. Kruse,¹⁴
 V. Krutelyov,⁵¹ S. E. Kuhlmann,² S. Kwang,¹² A. T. Laasanen,⁴⁶ S. Lai,³² S. Lami,⁴⁸ S. Lammel,¹⁵ J. Lancaster,¹⁴
 M. Lancaster,³⁰ R. Lander,⁶ K. Lannon,³⁸ A. Lath,⁵⁰ G. Latino,³⁶ R. Lauhakangas,²¹ I. Lazzizzera,⁴² Y. Le,²⁴ C. Lecci,²⁵
 T. LeCompte,² J. Lee,²⁷ J. Lee,⁴⁷ S. W. Lee,⁵¹ R. Lefèvre,³ N. Leonardo,³¹ S. Leone,⁴⁴ S. Levy,¹² J. D. Lewis,¹⁵ K. Li,⁵⁹
 C. Lin,⁵⁹ C. S. Lin,¹⁵ M. Lindgren,¹⁵ T. M. Liss,²³ A. Lister,¹⁸ D. O. Litvintsev,¹⁵ T. Liu,¹⁵ Y. Liu,¹⁸ N. S. Lockyer,⁴³
 A. Loginov,³⁵ M. Loretta,⁴² P. Loverre,⁴⁹ R-S. Lu,¹ D. Lucchesi,⁴² P. Lujan,²⁸ P. Lukens,¹⁵ G. Lungu,¹⁶ L. Lyons,⁴¹ J. Lys,²⁸
 R. Lysak,¹ D. MacQueen,³² R. Madrak,¹⁵ K. Maeshima,¹⁵ P. Maksimovic,²⁴ L. Malferrari,⁴ G. Manca,²⁹ R. Marginean,³⁸
 C. Marino,²³ A. Martin,⁵⁹ M. Martin,²⁴ V. Martin,³⁷ M. Martínez,³ T. Maruyama,⁵⁴ H. Matsunaga,⁵⁴ M. Mattson,⁵⁷
 P. Mazzanti,⁴ K. S. McFarland,⁴⁷ D. McGivern,³⁰ P. M. McIntyre,⁵¹ P. McNamara,⁵⁰ R. NeNulty,²⁹ A. Mehta,²⁹
 S. Menzemer,³¹ A. Menzione,⁴⁴ P. Merkel,¹⁵ C. Mesropian,⁴⁸ A. Messina,⁴⁹ T. Miao,¹⁵ N. Miladinovic,⁵ L. Miller,²⁰
 R. Miller,³⁴ J. S. Miller,³³ R. Miquel,²⁸ S. Miscetti,¹⁷ G. Mitselmakher,¹⁶ A. Miyamoto,²⁶ Y. Miyazaki,⁴⁰ N. Moggi,⁴
 B. Mohr,⁷ R. Moore,¹⁵ M. Morello,⁴⁴ P. A. Movilla Fernandez,²⁸ A. Mukherjee,¹⁵ M. Mulhearn,³¹ T. Muller,²⁵
 R. Mumford,²⁴ A. Munar,⁴³ P. Murat,¹⁵ J. Nachtman,¹⁵ S. Nahn,⁵⁹ I. Nakamura,⁴³ I. Nakano,³⁹ A. Napier,⁵⁵ R. Naporra,²⁴

- D. Naumov,³⁶ V. Necula,¹⁶ F. Niell,³³ J. Nielsen,²⁸ C. Nelson,¹⁵ T. Nelson,¹⁵ C. Neu,⁴³ M. S. Neubauer,⁸
 C. Newman-Holmes,¹⁵ T. Nigmanov,⁴⁵ L. Nodulman,² O. Norniella,³ K. Oesterberg,²¹ T. Ogawa,⁵⁶ S. H. Oh,¹⁴ Y. D. Oh,²⁷
 T. Ohsugi,²² T. Okusawa,⁴⁰ R. Oldeman,⁴⁹ R. Orava,²¹ W. Orejudos,²⁸ C. Pagliarone,⁴⁴ E. Palencia,¹⁰ R. Paoletti,⁴⁴
 V. Papadimitriou,¹⁵ S. Pashapour,³² J. Patrick,¹⁵ G. Pauletta,⁵³ M. Paulini,¹¹ T. Pauly,⁴¹ C. Paus,³¹ D. Pellett,⁶ A. Penzo,⁵³
 T. J. Phillips,¹⁴ G. Piacentino,⁴⁴ J. Piedra,¹⁰ K. T. Pitts,²³ C. Plager,⁷ A. Pompoš,⁴⁶ L. Pondrom,⁵⁸ G. Pope,⁴⁵ X. Portell,³
 O. Poukhov,¹³ F. Prakoshyn,¹³ T. Pratt,²⁹ A. Pronko,¹⁶ J. Proudfoot,² F. Ptahos,¹⁷ G. Punzi,⁴⁴ J. Rademacker,⁴¹
 M. A. Rahaman,⁴⁵ A. Rakitine,³¹ S. Rappoccio,²⁰ F. Ratnikov,⁵⁰ H. Ray,³³ B. Reisert,¹⁵ V. Rekovic,³⁶ P. Renton,⁴¹
 M. Rescigno,⁴⁹ F. Rimondi,⁴ K. Rinnert,²⁵ L. Ristori,⁴⁴ W. J. Robertson,¹⁴ A. Robson,⁴¹ T. Rodrigo,¹⁰ S. Rolli,⁵⁵
 L. Rosenson,³¹ R. Roser,¹⁵ R. Rossin,⁴² C. Rott,⁴⁶ J. Russ,¹¹ V. Rusu,¹² A. Ruiz,¹⁰ D. Ryan,⁵⁵ H. Saarikko,²¹ S. Sabik,³²
 A. Safonov,⁶ R. St. Denis,¹⁹ W. K. Sakamoto,⁴⁷ G. Salamanna,⁴⁹ D. Saltzberg,⁷ C. Sanchez,³ A. Sansoni,¹⁷ L. Santi,⁵³
 S. Sarkar,⁴⁹ K. Sato,⁵⁴ P. Savard,³² A. Savoy-Navarro,¹⁵ P. Schlabach,¹⁵ E. E. Schmidt,¹⁵ M. P. Schmidt,⁵⁹ M. Schmitt,³⁷
 L. Scodellaro,¹⁰ A. Scribano,⁴⁴ F. Scuri,⁴⁴ A. Sedov,⁴⁶ S. Seidel,³⁶ Y. Seiya,⁴⁰ F. Semeria,⁴ L. Sexton-Kennedy,¹⁵
 I. Sfiligoi,¹⁷ M. D. Shapiro,²⁸ T. Shears,²⁹ P. F. Shepard,⁴⁵ D. Sherman,²⁰ M. Shimojima,⁵⁴ M. Shochet,¹² Y. Shon,⁵⁸
 I. Shreyber,³⁵ A. Sidoti,⁴⁴ J. Siegrist,²⁸ M. Siket,¹ A. Sill,⁵² P. Sinervo,³² A. Sisakyan,¹³ A. Skiba,²⁵ A. J. Slaughter,¹⁵
 K. Sliwa,⁵⁵ D. Smirnov,³⁶ J. R. Smith,⁶ F. D. Snider,¹⁵ R. Snihur,³² A. Soha,⁶ S. V. Somalwar,⁵⁰ J. Spalding,¹⁵
 M. Spezziga,⁵² L. Spiegel,¹⁵ F. Spinella,⁴⁴ M. Spiropulu,⁹ P. Squillacioti,⁴⁴ H. Stadie,²⁵ B. Stelzer,³² O. Stelzer-Chilton,³²
 J. Strologas,³⁶ D. Stuart,⁹ A. Sukhanov,¹⁶ K. Sumorok,³¹ H. Sun,⁵⁵ T. Suzuki,⁵⁴ A. Taffard,²³ R. Tafirout,³² S. F. Takach,⁵⁷
 H. Takano,⁵⁴ R. Takashima,²² Y. Takeuchi,⁵⁴ K. Takikawa,⁵⁴ M. Tanaka,² R. Tanaka,³⁹ N. Tanimoto,³⁹ S. Tapprogge,²¹
 M. Tecchio,³³ P. K. Teng,¹ K. Terashi,⁴⁸ R. J. Tesarek,¹⁵ S. Tether,³¹ J. Thom,¹⁵ A. S. Thompson,¹⁹ E. Thomson,⁴³
 P. Tipton,⁴⁷ V. Tiwari,¹¹ S. Tkaczyk,¹⁵ D. Toback,⁵¹ K. Tollefson,³⁴ T. Tomura,⁵⁴ D. Tonelli,⁴⁴ M. Tönnesmann,³⁴
 S. Torre,⁴⁴ D. Torretta,¹⁵ S. Tourneur,¹⁵ W. Trischuk,³² J. Tseng,⁴¹ R. Tsuchiya,⁵⁶ S. Tsuno,³⁹ D. Tsybychev,¹⁶ N. Turini,⁴⁴
 M. Turner,²⁹ F. Ukegawa,⁵⁴ T. Unverhau,¹⁹ S. Uozumi,⁵⁴ D. Usynin,⁴³ L. Vacavant,²⁸ A. Vaiciulis,⁴⁷ A. Varganov,³³
 E. Vataga,⁴⁴ S. Vejcik III,¹⁵ G. Velev,¹⁵ V. Veszpremi,⁴⁶ G. Veramendi,²³ T. Vickey,²³ R. Vidal,¹⁵ I. Vila,¹⁰ R. Vilar,¹⁰
 I. Vollrath,³² I. Volobouev,²⁸ M. von der Mey,⁷ P. Wagner,⁵¹ R. G. Wagner,² R. L. Wagner,¹⁵ W. Wagner,²⁵ R. Wallny,⁷
 T. Walter,²⁵ T. Yamashita,³⁹ K. Yamamoto,⁴⁰ Z. Wan,⁵⁰ M. J. Wang,¹ S. M. Wang,¹⁶ A. Warburton,³² B. Ward,¹⁹
 S. Waschke,¹⁹ D. Waters,³⁰ T. Watts,⁵⁰ M. Weber,²⁸ W. C. Wester III,¹⁵ B. Whitehouse,⁵⁵ A. B. Wicklund,² E. Wicklund,¹⁵
 H. H. Williams,⁴³ P. Wilson,¹⁵ B. L. Winer,³⁸ P. Wittich,⁴³ S. Wolbers,¹⁵ C. Wolfe,¹² M. Wolter,⁵⁵ M. Worcester,⁷
 S. Worm,⁵⁰ T. Wright,³³ X. Wu,¹⁸ F. Würthwein,⁸ A. Wyatt,³⁰ A. Yagil,¹⁵ C. Yang,⁵⁹ U. K. Yang,¹² W. Yao,²⁸ G. P. Yeh,¹⁵
 K. Yi,²⁴ J. Yoh,¹⁵ P. Yoon,⁴⁷ K. Yorita,⁵⁶ T. Yoshida,⁴⁰ I. Yu,²⁷ S. Yu,⁴³ Z. Yu,⁵⁹ J. C. Yun,¹⁵ L. Zanello,⁴⁹ A. Zanetti,⁵³
 I. Zaw,²⁰ F. Zetti,⁴⁴ J. Zhou,⁵⁰ A. Zsenei,¹⁸ and S. Zucchelli⁴

(CDF Collaboration)

¹Institute of Physics, Academia Sinica, Taipei, Taiwan 11529, Republic of China²Argonne National Laboratory, Argonne, Illinois 60439, USA³Institut de Fisica d'Altes Energies, Universitat Autònoma de Barcelona, E-08193, Bellaterra (Barcelona), Spain⁴Istituto Nazionale di Fisica Nucleare, University of Bologna, I-40127 Bologna, Italy⁵Brandeis University, Waltham, Massachusetts 02254, USA⁶University of California at Davis, Davis, California 95616, USA⁷University of California at Los Angeles, Los Angeles, California 90024, USA⁸University of California at San Diego, La Jolla, California 92093, USA⁹University of California at Santa Barbara, Santa Barbara, California 93106, USA¹⁰Instituto de Fisica de Cantabria, CSIC-University of Cantabria, 39005 Santander, Spain¹¹Carnegie Mellon University, Pittsburgh, Pennsylvania 15213, USA¹²Enrico Fermi Institute, University of Chicago, Chicago, Illinois 60637, USA¹³Joint Institute for Nuclear Research, RU-141980 Dubna, Russia¹⁴Duke University, Durham, North Carolina 27708, USA¹⁵Fermi National Accelerator Laboratory, Batavia, Illinois 60510, USA¹⁶University of Florida, Gainesville, Florida 32611, USA¹⁷Laboratori Nazionali di Frascati, Istituto Nazionale di Fisica Nucleare, I-00044 Frascati, Italy¹⁸University of Geneva, CH-1211 Geneva 4, Switzerland¹⁹Glasgow University, Glasgow G12 8QQ, United Kingdom²⁰Harvard University, Cambridge, Massachusetts 02138, USA²¹The Helsinki Group: Helsinki Institute of Physics and Division of High Energy Physics, Department of Physical Sciences, University of Helsinki, FIN-00044, Helsinki, Finland²²Hiroshima University, Higashi-Hiroshima 724, Japan

²³*University of Illinois, Urbana, Illinois 61801, USA*²⁴*The Johns Hopkins University, Baltimore, Maryland 21218, USA*²⁵*Institut für Experimentelle Kernphysik, Universität Karlsruhe, 76128 Karlsruhe, Germany*²⁶*High Energy Accelerator Research Organization (KEK), Tsukuba, Ibaraki 305, Japan*²⁷*Center for High Energy Physics: Kyungpook National University, Taegu 702-701, Korea; Seoul National University, Seoul 151-742, Korea;**and SungKyunKwan University, Suwon 440-746, Korea*²⁸*Ernest Orlando Lawrence Berkeley National Laboratory, Berkeley, California 94720, USA*²⁹*University of Liverpool, Liverpool L69 7ZE, United Kingdom*³⁰*University College London, London WC1E 6BT, United Kingdom*³¹*Massachusetts Institute of Technology, Cambridge, Massachusetts 02139, USA*³²*Institute of Particle Physics: McGill University, Montréal, Canada H3A 2T8; and University of Toronto, Toronto, Canada M5S 1A7*³³*University of Michigan, Ann Arbor, Michigan 48109, USA*³⁴*Michigan State University, East Lansing, Michigan 48824, USA*³⁵*Institution for Theoretical and Experimental Physics, ITEP, Moscow 117259, Russia*³⁶*University of New Mexico, Albuquerque, New Mexico 87131, USA*³⁷*Northwestern University, Evanston, Illinois 60208, USA*³⁸*The Ohio State University, Columbus, Ohio 43210, USA*³⁹*Okayama University, Okayama 700-8530, Japan*⁴⁰*Osaka City University, Osaka 588, Japan*⁴¹*University of Oxford, Oxford OX1 3RH, United Kingdom*⁴²*University of Padova, Istituto Nazionale di Fisica Nucleare, Sezione di Padova-Trento, I-35131 Padova, Italy*⁴³*University of Pennsylvania, Philadelphia, Pennsylvania 19104, USA*⁴⁴*Istituto Nazionale di Fisica Nucleare, University and Scuola Normale Superiore of Pisa, I-56100 Pisa, Italy*⁴⁵*University of Pittsburgh, Pittsburgh, Pennsylvania 15260, USA*⁴⁶*Purdue University, West Lafayette, Indiana 47907, USA*⁴⁷*University of Rochester, Rochester, New York 14627, USA*⁴⁸*The Rockefeller University, New York, New York 10021, USA*⁴⁹*Istituto Nazionale di Fisica Nucleare, Sezione di Roma 1, University di Roma "La Sapienza," I-00185 Roma, Italy*⁵⁰*Rutgers University, Piscataway, New Jersey 08855, USA*⁵¹*Texas A&M University, College Station, Texas 77843, USA*⁵²*Texas Tech University, Lubbock, Texas 79409, USA*⁵³*Istituto Nazionale di Fisica Nucleare, University of Trieste/Udine, Italy*⁵⁴*University of Tsukuba, Tsukuba, Ibaraki 305, Japan*⁵⁵*Tufts University, Medford, Massachusetts 02155, USA*⁵⁶*Waseda University, Tokyo 169, Japan*⁵⁷*Wayne State University, Detroit, Michigan 48201, USA*⁵⁸*University of Wisconsin, Madison, Wisconsin 53706, USA*⁵⁹*Yale University, New Haven, Connecticut 06520, USA*

(Received 20 December 2004; published 16 March 2005)

We present measurements of the lifetimes and polarization amplitudes for $B_s^0 \rightarrow J/\psi\phi$ and $B_d^0 \rightarrow J/\psi K^{*0}$ decays. Lifetimes of the heavy and light mass eigenstates in the B_s^0 system are separately measured for the first time by determining the relative contributions of amplitudes with definite CP as a function of the decay time. Using 203 ± 15 B_s^0 decays we obtain $\tau_L = (1.05^{+0.16}_{-0.13} \pm 0.02)$ ps and $\tau_H = (2.07^{+0.58}_{-0.46} \pm 0.03)$ ps. Expressed in terms of the difference $\Delta\Gamma_s$ and average Γ_s , of the decay rates of the two eigenstates, the results are $\Delta\Gamma_s/\Gamma_s = (65^{+25}_{-33} \pm 1)\%$ and $\Delta\Gamma_s = (0.47^{+0.19}_{-0.24} \pm 0.01) \text{ ps}^{-1}$.

DOI: 10.1103/PhysRevLett.94.101803

PACS numbers: 13.25.Hw, 11.30.Er, 14.40.Nd

Particle-antiparticle oscillation occurs for both B_d^0 and B_s^0 mesons and gives rise, in each system, to two eigenstates with definite masses (heavy, m_H , and light, m_L) and widths (Γ_H and Γ_L). In the standard model (SM), this oscillation is due to second-order contributions from the weak interaction and depends on the Cabibbo-Kobayashi-Maskawa (CKM) quark mixing matrix. Oscillation has been observed in the B_d^0 system, and the mass difference ($\Delta m \equiv m_H - m_L$) is $\Delta m_d = (0.507 \pm 0.007) \text{ ps}^{-1}$ [1]. In the B_s^0 system, direct observation of the oscillation signal has been a challenge: the 95% C.L. limit for the mass

difference is $\Delta m_s > 14.4 \text{ ps}^{-1}$ [1]. The ratio of the decay width difference $\Delta\Gamma \equiv \Gamma_L - \Gamma_H$ to the average decay width $\Gamma \equiv (\Gamma_L + \Gamma_H)/2$ is expected to be small (0.2%–0.3%) for the B_d^0 system [2], but sizable for the B_s^0 system [3]. Reference [4] predicts $\Delta\Gamma_s/\Gamma_s = (12 \pm 6)\%$, and Ref. [5] gives the ratio of the decay width difference to the mass difference. If Δm_s is too large to be directly measured, a measurement of $\Delta\Gamma_s$ could serve instead, along with Δm_d , in tests of the unitarity of the CKM matrix. In the SM, the mass eigenstates in the B_s^0 system are expected to be nearly CP eigenstates. The light mass

eigenstate is expected to be CP even and to have a larger decay width, and thus a shorter lifetime, than the heavy mass eigenstate [6]. By exploiting decays with known CP content, it is possible to measure the two decay widths separately.

The decays $B_s^0 \rightarrow J/\psi\phi$ and $B_d^0 \rightarrow J/\psi K^{*0}$ (892) are pseudoscalar to vector-vector transitions and are characterized by three amplitudes. These amplitudes correspond to transitions in which the J/ψ and ϕ (or K^{*0}) have a relative orbital angular momentum L of 0, 1, or 2. In the transversity basis [6], the decay amplitudes correspond to linear polarization states of the vector mesons. The $L = 1$ decays take place via the decay amplitude A_{\perp} and correspond to a parity-odd (perpendicular) correlation between the transverse linear polarization states of the vector mesons. The other two decay amplitudes A_0 and A_{\parallel} lead to decays corresponding to linear combinations of the parity-even $L = 0$ and $L = 2$ decays. In this analysis, the fully reconstructed decays $B_s^0 \rightarrow J/\psi\phi$ (with $J/\psi \rightarrow \mu^+\mu^-$ and $\phi \rightarrow K^+K^-$) and $B_d^0 \rightarrow J/\psi K^{*0}$ (with $J/\psi \rightarrow \mu^+\mu^-$ and $K^{*0} \rightarrow K^+\pi^-$) and their charge conjugates are used to measure the polarization amplitudes. The observed final state particles for the B_s^0 and \bar{B}_s^0 decays ($\mu^+\mu^-K^+K^-$) have a definite CP , which depends on L , and a definite angular distribution. We determine the decay widths for the heavy and light B_s^0 mass eigenstates by measuring the relative contribution of the CP -odd and CP -even decays to the observed angular distribution as a function of the decay time. The B_d^0 decays provide a valuable control sample since they are expected to occur via similar (parity-odd and parity-even) decay amplitudes [6].

The analysis uses a portion of the data from run II at the Fermilab Tevatron $p\bar{p}$ collider, corresponding to an integrated luminosity of about 260 pb^{-1} . The data were collected with the upgraded Collider Detector at Fermilab (CDF) [7], the most relevant components of which are described below. A five-layer double-sided silicon micro-strip detector, SVX, provides track measurements at radii between 2.5 and 10.6 cm and allows for precise vertex reconstruction. A cylindrical drift chamber, COT, with eight alternating axial and stereo superlayers (each superlayer containing 12 sense wires) provides track measurements for charged particles between radii of 40 and 137 cm. The COT symmetry axis is the main axis of the cylindrical coordinate system used at CDF. Both tracking devices are immersed in a uniform axial 1.4 T magnetic field, allowing precision measurement of the momenta of charged particles in the radial direction p_T . Planar drift chambers located outside of calorimeters and additional steel absorbers are used to identify muons. Muons and charged hadrons are reconstructed in the central pseudo-rapidity region $|\eta| < 1$.

The three-level trigger system of CDF is used to select events of interest by requiring two oppositely charged particle tracks, each with $p_T > 1.5 \text{ GeV}/c$ and matched to hits in the muon detector. About $2.0 \times 10^6 J/\psi \rightarrow$

$\mu^+\mu^-$ signal candidates were selected by requiring a reconstructed mass within $80.0 \text{ MeV}/c^2$ of the J/ψ mass [1]. A B_s^0 (B_d^0) meson candidate is reconstructed by associating a J/ψ candidate with a pair of tracks, each with $p_T > 0.4 \text{ GeV}/c$, consistent with a $\phi \rightarrow K^+K^-$ ($K^{*0} \rightarrow K^+\pi^-$) decay. The K^+K^- ($K^+\pi^-$) mass is required to be within $6.5 \text{ MeV}/c^2$ ($50.0 \text{ MeV}/c^2$) of the ϕ (K^{*0}) pole mass [1]. When both $K^+\pi^-$ and π^+K^- particle assignments are kinematically viable in the K^{*0} reconstruction (no particle identification is used), the one giving the mass closest to the pole K^{*0} mass is chosen. This reduces the contribution from candidates with swapped particle assignment down to about 10% of the total signal. Background is suppressed by requiring $p_T(B_{s,d}^0) > 6.0 \text{ GeV}/c$, $p_T(\phi) > 2.0 \text{ GeV}/c$, and $p_T(K^{*0}) > 2.6 \text{ GeV}/c$. The more restrictive cut on $p_T(K^{*0})$ is determined by an optimization procedure, and is a consequence of the larger combinatorial background underneath the K^{*0} peak.

We fit the B candidates subject to the constraint that the four tracks originate from a common point. In order to improve the mass resolution, the $\mu^+\mu^-$ mass is constrained to the J/ψ mass. To ensure only well measured vertices, a set of track and vertex quality requirements is applied [8]. In particular, all four tracks are required to have measurements in at least three axial layers of the silicon detector. The proper decay time, t , is determined from the radial distance l_T from the beam axis to the B meson decay vertex, signed relative to the direction of \vec{p}_T of the B candidate: $ct = c(l_T \cdot \vec{p}_T)M_B/p_T^2$. The position of the beam axis is determined using data taken with an inclusive jet trigger. The radial profile of the beam is approximately Gaussian with a rms of about $30 \mu\text{m}$.

In the B_d^0 system, the mass eigenstates are not CP eigenstates, and the observed decays are flavor specific with the charge of the K meson identifying whether the decay is that of a B_d^0 or a \bar{B}_d^0 . Summing over initially produced B_d^0 and \bar{B}_d^0 yields a differential decay rate [9] which is insensitive to first order to a lifetime difference [2]:

$$\begin{aligned} \frac{d^4\mathcal{P}(\vec{\rho}, t)}{d\vec{\rho}dt} \propto & [|A_0|^2 \cdot f_1(\vec{\rho}) + |A_{\parallel}|^2 \cdot f_2(\vec{\rho}) \\ & + |A_{\perp}|^2 \cdot f_3(\vec{\rho}) \pm \text{Im}(A_{\parallel}^* A_{\perp}) \cdot f_4(\vec{\rho}) \\ & + \text{Re}(A_0^* A_{\parallel}) \cdot f_5(\vec{\rho}) \pm \text{Im}(A_0^* A_{\perp}) \cdot f_6(\vec{\rho})] e^{-\Gamma_d t}. \end{aligned}$$

Here the upper (lower) sign is used for $K^+\pi^-$ ($K^-\pi^+$) in the final state and $\Gamma_d \equiv 1/\tau_{B_d^0}$. The functions $f_i(\vec{\rho})$ depend on the transversity variables $\vec{\rho} \equiv \{\cos\theta, \varphi, \cos\psi\}$, all of which are defined in Ref. [9].

In the B_s^0 system, the SM expectation is that CP violation due to mixing is small, and the mass eigenstates are nearly CP eigenstates. Ignoring CP violation due to mixing, and summing the distributions for initially produced B_s^0 and \bar{B}_s^0 mesons, the interference terms between the CP -even and CP -odd amplitudes cancel, leaving

$$\frac{d^4 \mathcal{P}(\vec{\rho}, t)}{d\vec{\rho} dt} \propto |A_0|^2 e^{-\Gamma_L t} \cdot f_1(\vec{\rho}) + |A_{||}|^2 e^{-\Gamma_L t} \cdot f_2(\vec{\rho}) + |A_{\perp}|^2 e^{-\Gamma_H t} \cdot f_3(\vec{\rho}) + \text{Re}(A_0^* A_{||}) \cdot f_5(\vec{\rho}) e^{-\Gamma_L t}.$$

In the B_s^0 analysis, the observed final states have definite CP which depends on L . The CP -even angular decay terms ($A_{0,||}$) evolve in time as $e^{-\Gamma_L t}$, while the CP -odd angular decay terms (A_{\perp}) evolve as $e^{-\Gamma_H t}$.

For both B_d^0 and B_s^0 decays, the amplitudes are normalized so that $|A_0|^2 + |A_{||}|^2 + |A_{\perp}|^2 = 1$, and an unobservable overall phase is removed by setting $\arg(A_0) = 0$. The decay amplitudes are assumed to be CP conserving.

An unbinned likelihood fit is performed to mass, ct , and $\vec{\rho}$ in order to extract the decay amplitudes $A_{0,||,\perp}$ and decay widths Γ (Γ_H and Γ_L in the case of the B_s^0). Inclusion of the mass information in the fit is crucial for separation of the signal from the background. The mass distribution is modeled with a Gaussian for the signal peak and a linear shape for the background. The mass-measurement uncertainty is incorporated for each candidate. The probability density function for ct includes positive exponentials for the signal, a δ function for the prompt background (which is about 85% of the total) and a set of exponentials for positive and negative decay lengths which describe a short-lived background component due to mismeasured vertices and a long-lived contribution due to incorrectly reconstructed heavy-flavor decays. Each contribution is convoluted with a Gaussian resolution function, the width of which is proportional to the uncertainty of the candidate's ct measurement. To allow for a systematic underestimate of the uncertainties, the mass and the ct uncertainties are multiplied by scale factors determined in the fit. The $\vec{\rho}$ distribution of the signal is parametrized in accordance with the equations above. The background distributions in ct and $\vec{\rho}$ are assumed to be uncorrelated. The latter is described by a shape similar to that of the signal, but with an independent set of amplitudes. The relationship of mass, ct , and $\vec{\rho}$ of the B_d^0 candidates with $K\pi$ misassignment to those of correctly reconstructed candidates is established via Monte Carlo simulation.

Distributions in $\vec{\rho}$ are distorted by the detector acceptance, the trigger efficiency, and, most importantly, the kinematic selection criteria. We use the method developed for the CDF run I measurement of transversity amplitudes [10,11] to account for this distortion. With as little as six constants extracted from Monte Carlo decays generated uniformly in $\vec{\rho}$, this method allows one to avoid the need for explicit parametrization of the distortion in the likelihood. All aspects of the fitting are extensively verified using Monte Carlo simulations.

Data and fit projections in mass and ct for the B_s^0 and B_d^0 are shown in Figs. 1 and 2. Fits in the transversity subspace are illustrated by Fig. 3.

The single largest source of systematic uncertainty in the measurement of the transversity amplitudes of B_d^0 and B_s^0 is the choice of parametrization of the background distribu-

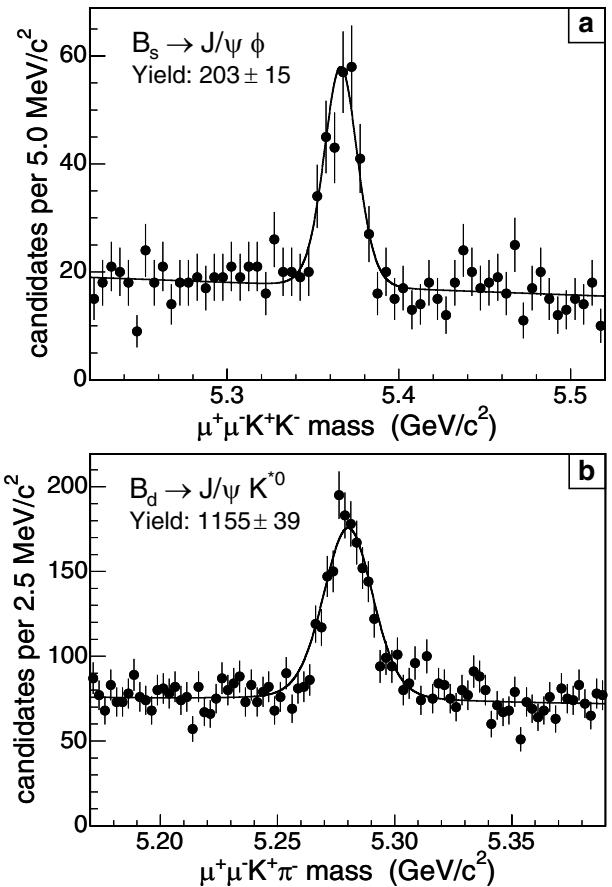


FIG. 1. Mass distribution with the fit projection overlaid: (a) $B_s^0 \rightarrow J/\psi \phi$; (b) $B_d^0 \rightarrow J/\psi K^{*0}$.

tion in $\vec{\rho}$. The B_s^0 transversity amplitudes receive a small contribution to their systematic uncertainty from a 3.5% contamination from B_d^0 . Two other sources contribute to the uncertainty in B_d^0 amplitudes: the way candidates with incorrect $K\pi$ assignment are handled and the potential contribution of $\mu^+ \mu^- K^+ \pi^-$ final states that are not due to $B_d^0 \rightarrow J/\psi K^{*0}(892)$ decays, which is estimated to be less than 4% of the total signal. The systematic uncertainty in the lifetimes receives contributions from the choice of the ct parametrization and from the SVX alignment. Slightly larger contributions come from the choice of the background parametrization in $\vec{\rho}$ and, in the case of B_s^0 , from B_d^0 contamination. For $\Delta\Gamma_s/\Gamma_s$ the only two sources of systematic uncertainty are from the choice of the background $\vec{\rho}$ parametrization and from B_d^0 contamination. Other potential sources of systematic uncertainty, including those from the method of correcting for distortion of the signal distribution in $\vec{\rho}$ and potential contribution of $B_s^0 \rightarrow J/\psi f^0(980)$ decays, were found to be negligible. The precision of all of the results of this analysis is statistically limited.

Results from the time-dependent angular analysis are given in Table I. The B_d^0 decay amplitudes and phases are of comparable precision and in agreement with results from BABAR [12] and Belle [13], and the lifetime is in

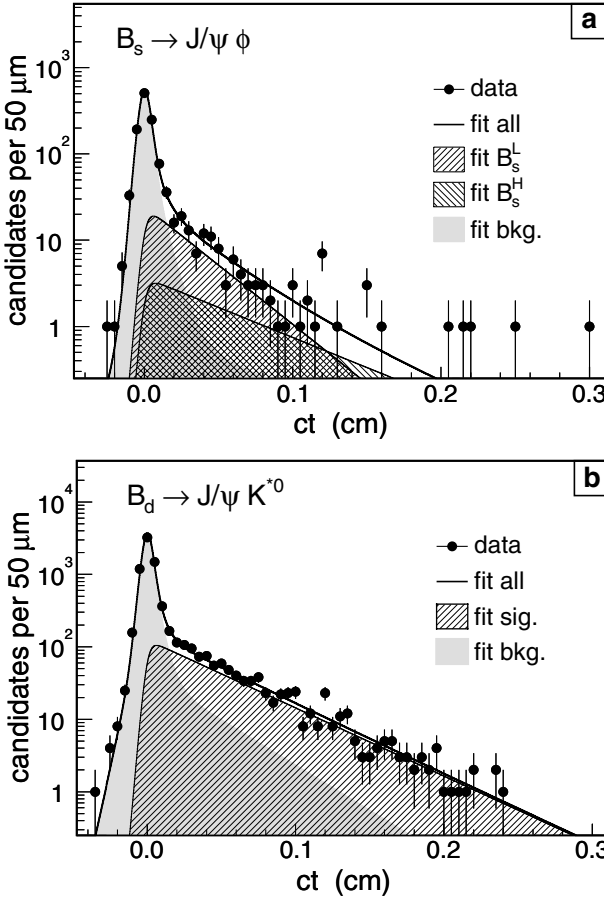


FIG. 2. ct distribution with the fit projection for the signal and background (bkg.) overlaid: (a) $B_s^0 \rightarrow J/\psi \phi$; (b) $B_d^0 \rightarrow J/\psi K^{*0}$.

agreement with the world average value [1]. Previous results [11] for the B_s^0 decay amplitudes, obtained from a time-integrated analysis, are in agreement with the results obtained in this analysis. Within uncertainties, the amplitudes for the B_s^0 and B_d^0 decays are in agreement, as is

expected in the limit of $SU(3)$ flavor symmetry [9]. Explicitly requiring exact $SU(3)$ symmetry by setting the B_s^0 decay amplitudes to be equal to those of the B_d^0 gives a consistent result for $\Delta\Gamma_s/\Gamma_s$ within uncertainties.

It is predicted [3] that the B_d^0 and B_s^0 total decay widths should be equal to within 1%. This expectation can be used as a constraint in the B_s^0 fit by requiring $1/\Gamma_s \equiv \tau_{B_s^0} = 2\tau_H\tau_L/(\tau_H + \tau_L) = \tau_{B_d^0} \equiv 1/\Gamma_d$, with $c\tau_{B_d^0} = 460.8 \pm 4.2 \mu\text{m}$, the known value for the B_d^0 lifetime [1] with an additional 1% uncertainty added in quadrature. By applying this constraint in the fit, we find $\Delta\Gamma_s/\Gamma_s = (71^{+24}_{-28} \pm 1)\%$ and $\Delta\Gamma_s = (0.46^{+0.17}_{-0.18} \pm 0.01) \text{ ps}^{-1}$. Although the uncertainties are still sizable, the fits with and without the $\Gamma_s = \Gamma_d$ constraint favor a nonzero value for $\Delta\Gamma_s/\Gamma_s$.

Monte Carlo methods are employed to estimate the probability for an experiment with similar statistical sensitivity to yield $\Delta\Gamma_s/\Gamma_s$ as large as is observed in this analysis. For the SM expectation, $\Delta\Gamma_s/\Gamma_s = 12\%$, one experiment in 84 (204) would give a result larger than that obtained from the unconstrained (constrained) fit. If no lifetime difference were expected, $\Delta\Gamma_s/\Gamma_s = 0$, one experiment in 315 (718) would give a result larger than that obtained from the unconstrained (constrained) fit.

A lifetime difference should result in an increase of the fraction of CP -odd $B_s^0 \rightarrow J/\psi \phi$ decays obtained in a time-integrated angular fit as a function of a cut on ct . The time-integrated CP -odd fraction extracted from fits for four values of the ct cut are shown in the second column of Table II. Using $c\tau_L$ and $c\tau_H$ obtained from the time-dependent fit and the observation that the time-integrated CP -odd fraction is 20% for $ct > 0$, one obtains expected fractions for the other ct cuts, shown in the third column in Table II, which are in agreement with the observations. The $B_d^0 \rightarrow J/\psi K^{*0}$ decays provide an important cross-check of the results obtained for the $B_s^0 \rightarrow J/\psi \phi$ decays. Fits for the time-integrated fraction of parity-odd B_d^0 decays show, as

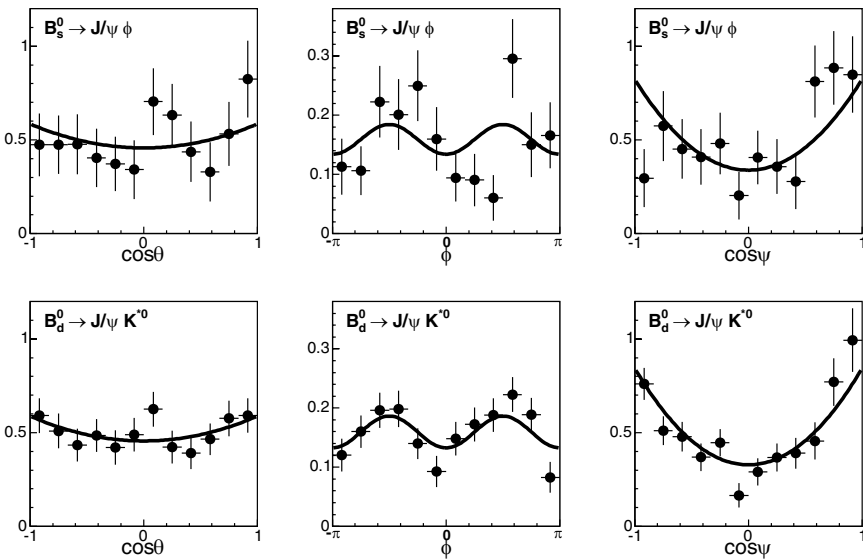


FIG. 3. Projections of the fit onto transversity variables for the mass-sideband-subtracted acceptance-corrected signal: $B_s^0 \rightarrow J/\psi \phi$ (top row); $B_d^0 \rightarrow J/\psi K^{*0}$ (bottom row). A $ct > 0$ cut is applied.

TABLE I. Summary of the results of the time-dependent angular analysis of $B_s^0 \rightarrow J/\psi\phi$ and $B_d^0 \rightarrow J/\psi K^{*0}$ decays. A measurement of $\arg(A_\perp)$ is not possible for the B_s^0 decays because the final state particles do not distinguish the decay of a B_s^0 from that of a \bar{B}_s^0 . For the B_s^0 decays, any pair of quantities describing signal lifetimes ($\tau_{B_s^0} = 1/\Gamma_s$, τ_H , τ_L , $\Delta\Gamma_s/\Gamma_s$, and $\Delta\Gamma_s$) may be used as free parameters in a fit; separate fits using different pairs are performed to obtain directly the results and asymmetric (statistical) uncertainties for each of the quantities.

	B_s^0	B_d^0
N_{sig}	203 ± 15	1155 ± 39
A_0	$0.784 \pm 0.039 \pm 0.007$	$0.750 \pm 0.017 \pm 0.012$
$ A_{\parallel} $	$0.510 \pm 0.082 \pm 0.013$	$0.473 \pm 0.034 \pm 0.006$
$ A_{\perp} $	$0.354 \pm 0.098 \pm 0.003$	$0.464 \pm 0.035 \pm 0.007$
$\arg(A_{\parallel})$	$1.94 \pm 0.36 \pm 0.03$	$2.86 \pm 0.22 \pm 0.07$
$\arg(A_{\perp})$		$0.15 \pm 0.15 \pm 0.04$
$c\tau_{B_d^0}$		$(462 \pm 15 \pm 6) \mu\text{m}$
$c\tau_{B_s^0}$	$(419_{-38}^{+45} \pm 6) \mu\text{m}$	
$c\tau_L$	$(316_{-40}^{+48} \pm 6) \mu\text{m}$	
$c\tau_H$	$(622_{-138}^{+175} \pm 9) \mu\text{m}$	
$\Delta\Gamma_s/\Gamma_s$		$(65_{-33}^{+25} \pm 1)\%$
$\Delta\Gamma_s$	$(0.47_{-0.24}^{+0.19} \pm 0.01) \text{ ps}^{-1}$	

expected, that the fraction remains unchanged with respect to cuts on ct (last column of Table II). In addition, a fit of the B_d^0 data can be performed allowing two lifetime components. The results are consistent with no lifetime difference for the full sample [$\Delta\Gamma/\Gamma = (15 \pm 12)\%$], as well as for independent subsamples having a statistical sensitivity similar to the B_s^0 decay sample. This result is not a measurement of a lifetime difference in the B_d^0 system, but is rather a cross-check of the analysis technique.

In conclusion, we have performed the first time-dependent angular analysis of $B_s^0 \rightarrow J/\psi\phi$ decays and have performed a similar measurement with $B_d^0 \rightarrow J/\psi K^{*0}$ decays. The measured B_d^0 polarization amplitudes are of comparable precision to, and in agreement with,

TABLE II. Time-integrated CP -odd B_s^0 and parity-odd B_d^0 fractions (in %) vs a cut on the decay length, ct .

ct cut	B_s^0 fitted	B_s^0 expected	B_d^0 fitted
$>0 \mu\text{m}$	20 ± 9	20 (reference)	22 ± 4
$>150 \mu\text{m}$	24 ± 10	24	23 ± 4
$>300 \mu\text{m}$	30 ± 13	29	23 ± 4
$>450 \mu\text{m}$	39 ± 12	34	24 ± 5

previously published results. The measured B_s^0 polarization amplitudes are the most precise available. Analysis of the $B_s^0 \rightarrow J/\psi\phi$ decays indicates a nonzero lifetime difference between the heavy and light mass eigenstates of the B_s^0 system. The result obtained, $\Delta\Gamma_s/\Gamma_s = (65_{-33}^{+25} \pm 1)\%$, has a central value larger than the SM expectation of $(12 \pm 6)\%$.

We thank the Fermilab staff and the technical staffs of the participating institutions for their vital contributions. This work was supported by the U.S. Department of Energy and National Science Foundation; the Italian Istituto Nazionale di Fisica Nucleare; the Ministry of Education, Culture, Sports, Science, and Technology of Japan; the Natural Sciences and Engineering Research Council of Canada; the National Science Council of the Republic of China; the Swiss National Science Foundation; the A.P. Sloan Foundation; the Bundesministerium fuer Bildung und Forschung, Germany; the Korean Science and Engineering Foundation and the Korean Research Foundation; the Particle Physics and Astronomy Research Council and the Royal Society, U.K.; the Russian Foundation for Basic Research; the Comision Interministerial de Ciencia y Tecnologia, Spain; and in part by the European Community's Human Potential Programme under Contract No. HPRN-CT-20002, Probe for New Physics.

- [1] S. Eidelman *et al.*, Phys. Lett. B **592**, 1 (2004).
- [2] A. Dighe, T. Hurth, C. Kim, and T. Yoshikawa, Nucl. Phys. **B624**, 377 (2002).
- [3] I. Bigi *et al.*, in *B Decays*, edited by S. Stone (World Scientific, Singapore, 1994), 2nd ed.
- [4] I. Dunietz, R. Fleischer, and U. Nierste, Phys. Rev. D **63**, 114015 (2001).
- [5] M. Beneke *et al.*, Phys. Lett. B **459**, 631 (1999).
- [6] A. S. Dighe, I. Dunietz, H. J. Lipkin, and J. L. Rosner, Phys. Lett. B **369**, 144 (1996).
- [7] CDF Collaboration, Fermilab Report No. FERMILAB-PUB-04-440-E, 2004.
- [8] K. Anikeev, Ph.D. thesis, MIT (Institution Report No. FERMILAB-THESIS-2004-12, 2004).
- [9] A. Dighe, I. Dunietz, and R. Fleischer, Eur. Phys. J. C **6**, 647 (1999).
- [10] S. Pappas, Ph.D. thesis, Yale University (Institution Report No. FERMILAB-THESIS-1999-48, 1999).
- [11] CDF Collaboration, T. Affolder *et al.*, Phys. Rev. Lett. **85**, 4668 (2000).
- [12] BABAR Collaboration, B. Aubert *et al.*, Phys. Rev. Lett. **87**, 241801 (2001).
- [13] Belle Collaboration, K. Abe *et al.*, Phys. Lett. B **538**, 11 (2002).